Hyperfine Interact
DOI 10.1007/s10751-012-0702-8

Effect of Co^{2+} content on the magnetic properties of $Co_xFe_{3-x}O_4/SiO_2$ nanocomposites

J. Hua · M. Liu · L. Wang · S. C. Xu · M. Feng · H. B. Li

Abstract Non-stoichiometric $Co_xFe_{3-x}O_4/SiO_2$ (x = 0.8, 0.9, 1.0, 1.1) nanocomposites have been prepared by sol-gel method. The structure, morphology and magnetic properties of the obtained samples were characterized by X-ray diffraction, transmission electron microscopy, vibrating sample magnetometer and Mössbauer spectroscopy at room temperature. As the Co^{2+} content increases, the average particle size of the spherical $Co_xFe_{3-x}O_4$ in the samples decreases and the lattice constants increases. The hyperfine fields for both A- and B-site decrease, while the fraction of Co^{2+} occupying the A-site increases. Magnetization measurements show the saturation magnetization and coercivity of $Co_xFe_{3-x}O_4/SiO_2$ decrease with increasing Co^{2+} content. The decrease in magnetization results from the weakened A-B interactions between Fe^{3+}, and the change in coercivity can be related to the variation of Co^{2+} at B-site and the decreasing particle size.

Keywords Sol-gel method · Nanocomposites · Mössbauer spectroscopy · Magnetic properties

1 Introduction

Nanosized cobalt ferrite ($CoFe_2O_4$) crystallizes in a partially inverse spinel structure and exhibits very high magnetocrystalline anisotropy, high coercivity, moderate saturation magnetization, remarkable chemical stability [1–3]. These properties make it a good candidate for high-density magnetic recording media. Most of these properties

J. Hua · M. Liu · L. Wang · S. C. Xu · M. Feng · H. B. Li (✉)
Key Laboratory of Functional Materials Physics and Chemistry of the Ministry of Education, Jilin Normal University, Siping 136000, China
e-mail: lihaibo@jlnu.edu.cn

J. Hua · H. B. Li
State Key Laboratory of Inorganic Synthesis and Preparative Chemistry, Jilin University, Changchun 130012, China

Published online: 17 November 2012

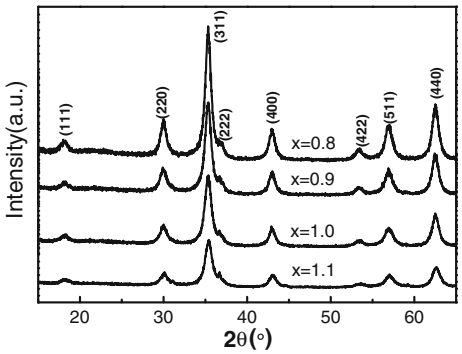

Fig. 1 XRD patterns of $Co_xFe_{3-x}O_4/SiO_2$ samples with different Co^{2+} content

are strongly dependent on both the size and composition of the nanoparticles, which are closely related to the method of preparation [4–8]. Cedeño-Mattei and co-worker [8] have prepared cobalt ferrite nanocrystals at various Fe:Co mole ratios (3:1, 2:1, 1.7:1, and 1.4:1) and found the grain size decreased while the coercivity value increased with increasing Fe:Co mole ratio.

The synthesis of nanocomposites formed by magnetic nanoparticles dispersed in amorphous matrix is an effective method to control particle size and magnetic properties as well as avoid agglomeration of magnetic particles. This makes it very easy to exploit the physical and chemical properties of magnetic materials. On the other hand,the sol–gel method is introduced as a versatile technique to prepare nanocomposites. The advantages of this route are relatively low preparation temperature and high reactive activity, and the as-synthesized materials have homogeneity and accurate composition [9, 10]. In the present paper, a series of nanocomposites were obtained by the dispersion of $Co_xFe_{3-x}O_4$ particles in an amorphous sillica matrix using sol-gel method, and X-ray diffractometer (XRD), transmission electron microscopy (TEM), vibrating sample magnetometer (VSM) and Mössbauer spectroscopy were used to investigate the effect of Co^{2+} content on the structure and magnetic properties of $Co_xFe_{3-x}O_4/SiO_2$ nanocomposites.

2 Experimental

Nanocomposites of $Co_xFe_{3-x}O_4/SiO_2$ (x = 0.8, 0.9, 1.0, 1.1) were prepared by the sol–gel process using metallic nitrates, $Co(NO_3)_2{\cdot}6H_2O$, $Fe(NO_3)_3{\cdot}9H_2O$ and tetraethylorthosilicate $Si(OC_2H_5)_4$ (TEOS) as precursors. The mass ration of SiO_2 and $Co_xFe_{3-x}O_4$ was 3:7. For the sample preparation, raw materials were dissolved in deionized water to form a mixed solution, adding the alcoholic solution of $Si(OC_2H_5)_4$ and drops of HNO_3. After adequate stirring for 1 h, the sol was heated to 60° in order to obtain it as a gel. The obtained gels were put into a drying oven for further drying at 100° for 24 h to obtain xerogels. The xerogels were annealed at 900° for 2 h in air to form $Co_xFe_{3-x}O_4/SiO_2$ nanocomposites.

The structure and crystallite sizes of the samples were characterized by XRD using a Rigaku D/max-2500 diffractometer with Cu Kα_1 radiation. High-purity silicon powders were used as a standard sample to determine the average particle sizes and lattice constants, which were determined from the X-ray data using MDI Jade 6.5

Table 1 Crystalline sizes and lattice constants of $Co_xFe_{3-x}O_4$ in $Co_xFe_{3-x}O_4/SiO_2$ samples

X	0.8	0.9	1.0	1.1
D (nm)	10.1	9.4	8.7	7.3
a_0 (nm)	0.8361	0.8366	0.8376	0.8381

software. The morphology and sizes of the samples were observed by using JEM-2100HR TEM apparatus. The magnetic properties of the samples were measured at room temperature using a Lake Shore 7407 VSM with a maximum applied field of 20 kOe. The ^{57}Fe Mössbauer spectra were collected on a FAST Comtec Mössbauer Systems at room temperature, using a $^{57}Co(Pd)$ source and a conventional constant acceleration mode. A high purity α-Fe foil was used for velocity calibration. The spectra were fitted with Lorentzian lines via the least squares method.

3 Results and discussions

3.1 XRD and TEM analyses

Figure 1 shows the XRD patterns of $Co_xFe_{3-x}O_4/SiO_2$ (x = 0.8, 0.9, 1.0, 1.1) samples. The diffraction peaks from (111), (220), (311), (222), (400), (422), (511), and (440) crystal plane observed in Fig. 1 confirm that $Co_xFe_{3-x}O_4$ in the sample have a spinel structure and the major peaks match with the standard pattern of bulk $CoFe_2O_4$ (JCPDS 22-1086). There is no other phase present in the cobalt rich sample (x = 1.1), indicating that the excess Co^{2+} might be incorporated into the Co-ferrite forming a cobalt rich spinel ferrite ($Co_{1.1}Fe_{1.9}O_4$). Any reflection from SiO_2 is not detected in the XRD patterns, demonstrating that SiO_2 remains amorphous in these composites. The average grain sizes D and lattice constants a_0 obtained for $Co_xFe_{3-x}O_4$ using XRD data are listed in Table 1. As x increases from 0.8 to 1.1, the average particle size of $Co_xFe_{3-x}O_4$ in the samples decreases from 10.1 to 7.3 nm, indicating that more Co^{2+} content would restrain the growth of $Co_xFe_{3-x}O_4$. Another observation is that the lattice constant increases with increasing Co^{2+} content. The increase in lattice constant can be attributed to the replacement of the smaller ionic radius of Fe^{3+} (0.064 nm) by the larger Co^{2+} (0.074 nm).

In Fig. 2a a TEM image of $Co_{0.8}Fe_{2.2}O_4/SiO_2$ sample is shown and it can be observed that $Co_{0.8}Fe_{2.2}O_4$ nanoparticles appear to be nearly spherical in shape and have a size distribution with an average size of 9.5 nm estimated by a statistical method, which is consistent with the calculated results from XRD pattern. Continuous lattice fringes could be clearly observed in the high-resolution transmission electron microscopy (HRTEM) image shown in Fig. 2b, indicating the high crystallinity of $Co_{0.8}Fe_{2.2}O_4$ nanocrystals are surrounded by amorphous SiO_2.

3.2 Mössbauer spectra analyses

The Mössbauer spectra of the $Co_xFe_{3-x}O_4/SiO_2$ samples, shown in Fig. 3, are consisted of a broad line sextet and an acceptable fit was obtained when the data was fitted with three magnetic components, and the Mössbauer parameters are listed

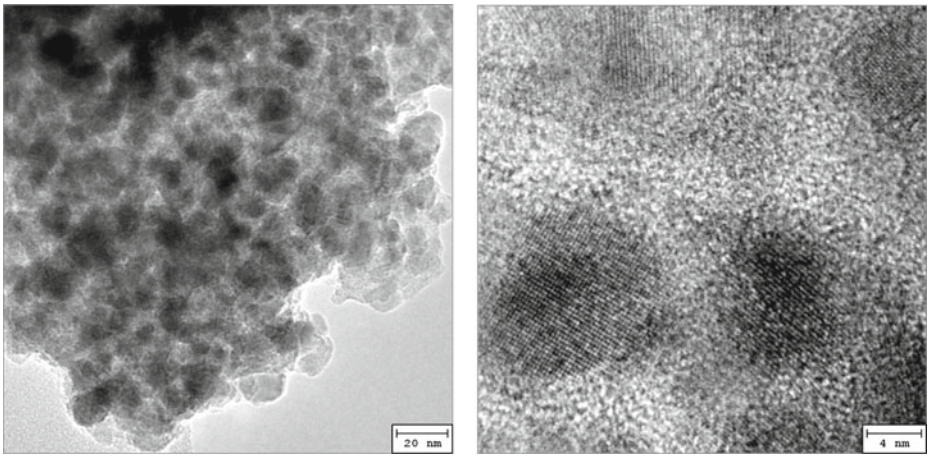

Fig. 2 TEM (**a**) and HRTEM (**b**) images of $Co_{0.8}Fe_{2.2}O_4/SiO_2$ sample

Fig. 3 Mössbauer spectra of $Co_xFe_{3-x}O_4/SiO_2$ samples with different Co^{2+} contents

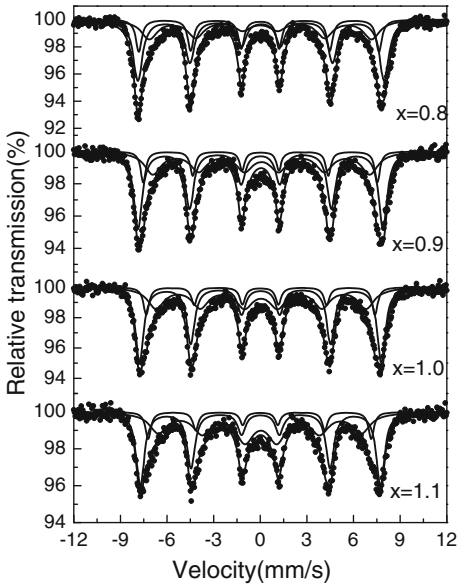

in Table 2. The IS values varied in the range of 0.28–0.40 mm/s are consistent with the high spin Fe^{3+} state [11].

For the three magnetic sextets, the component A with the smaller hyperfine field is assigned to the Fe^{3+} occupying A-site, the component B with the largest hyperfine field is assigned to the Fe^{3+} occupying B-site, and the component C with the smallest hyperfine field may be attributed to the Fe^{3+} on the surface layer, in which spins exhibit canting and disorder due to broken exchange bonds on the surface [12]. As the Co^{2+} content increases from 0.8 to 1.1, the fraction in component C increases

Table 2 Mössbauer parameters of $Co_xFe_{3-x}O_4/SiO_2$ samples with different Co^{2+} content

Sample	Component	IS (mm/s)	QS (mm/s)	HIN (kOe)	HWHM (mm/s)	AREA (%)	$R(S_A/S_A+S_B)$ (%)
X = 0.8	sextet(A)	0.284	0.085	479	0.23	21.7	31.1
	sextet(B)	0.384	0.010	491	0.36	48.0	
	sextet(C)	0.330	−0.013	444	0.64	30.3	
0.9	sextet(A)	0.337	0.014	466	0.19	14.4	22.4
	sextet(B)	0.343	−0.010	488	0.32	49.8	
	sextet(C)	0.394	−0.017	432	0.64	35.8	
1.0	sextet(A)	0.347	0.013	456	0.22	13.5	21.6
	sextet(B)	0.376	0.002	482	0.31	48.8	
	sextet(C)	0.319	−0.005	419	0.64	37.7	
1.1	sextet(A)	0.310	0.037	445	0.21	11.6	20.6
	sextet(B)	0.340	−0.01	479	0.31	44.6	
	sextet(C)	0.330	0.067	405	0.68	43.7	

IS is the isomer shift; QS is the quadruple split; HIN is the magnetic hyperfine field; HWHM is the half width at half maximum, and AREA is the absorption area

from 30.2 % to 43.7 %, indicating the fraction of surface noncollinear layer increases with a gradual decrease in grain size because of the surface effect and small size effect [13]. The result is well correlated with the results obtained from XRD analysis.

The peak area variation of A- and B-site reflects the situation of migrating cations. Table 2 shows that the area ratio $R = S_A/(S_A + S_B)$ of the A and B subspectra. As the content of Co^{2+} increases from 0.8 to 1.1, the value of R decreases from 30.1 % to 20.6 %, which indicates that the percentage occupation of magnetic Fe^{3+} at A-site decreases while that of Co^{2+} increases.

From Table 2, it can be seen that the magnetic hyperfine fields (HIN) at the A- and B-site decrease with increasing Co^{2+} content. According to Neel's model, the (A-B) inter-sublattice superexchange interactions of the magnetic cations are much stronger than the (A-A) and (B-B) intra-sublattice exchange interactions in the spinel lattice systems (AB_2O_4). In our experiments, as Fe^{3+} and Co^{2+} are occupying on both A and B sites, the following interactions are mainly to be considered:

$$Fe^{3+}_{A-}O^{2-}Fe^{3+}_{B},\ Fe^{3+}_{A-}O^{2-}Co^{2+}_{B},\ Co^{2+}_{A-}O^{2-}Fe^{3+}_{B}$$

Among the three interactions, the net magnetic field is mainly induced by the strong A-B interactions between Fe^{3+}. As Co^{2+} increases by replacing Fe^{3+}, the number of magnetic linkages in Fe^{3+}_{A}-$O^{2-}Fe^{3+}_{B}$ decreases. Thus, the hyperfine fields are expected to decrease with increasing Co^{2+} content.

3.3 VSM analyses

Figure 4 shows the hysteresis loops of $Co_xFe_{3-x}O_4/SiO_2$ samples. All samples exhibit typical ferromagnetic behaviors. The inset in Fig. 4 shows the hysteresis loops measured at the range of approximately −800 to +800 Oe for clear visibility. The Magnetic parameters for all samples are listed in Table 3. The values of the saturation magnetization *Ms* were obtained by extrapolation to infinite field in a M vs. $1/H^2$ plot [14, 15] (shown in Fig. 5). Compared with the $CoFe_2O_4$ nanoparticles studied by Lee et al. [16], the lower magnetization value for all samples results from weak

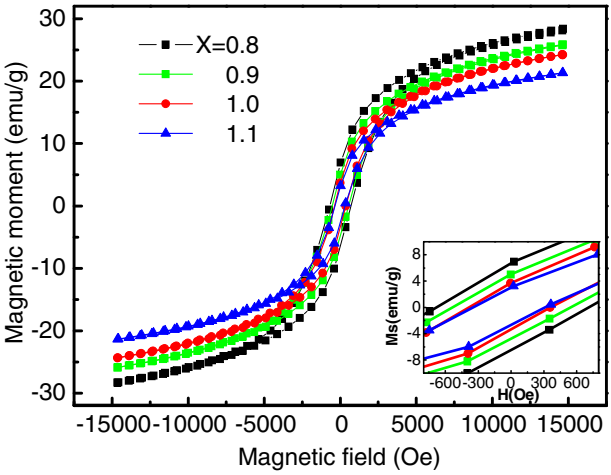

Fig. 4 Room temperature hysteresis loops of $Co_xFe_{3-x}O_4/SiO_2$ composites with different Co^{2+} content (The inset shows the hysteresis loops measured at the range of approximately −800 to +800 Oe)

Table 3 Magnetic parameters of $Co_xFe_{3-x}O_4/SiO_2$ samples

X	0.8	0.9	1.0	1.1
Hc (Oe)	696	538	371	328
Ms (emu/g)	29.8	27.6	25.9	22.5

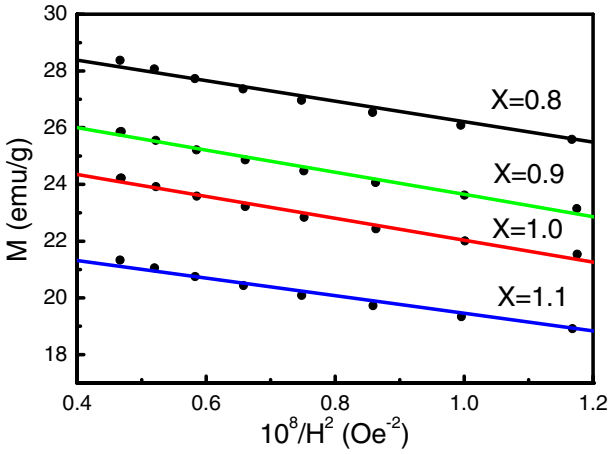

Fig. 5 Variation of the magnetization M with $1/H^2$

exchange interaction between $Co_xFe_{3-x}O_4$ grains because amorphous SiO_2 exists in the boundaries around $Co_xFe_{3-x}O_4$ grains.

It can be seen that as the Co^{2+} content increases from 0.8 to 1.1, the saturation magnetization Ms and coerivity Hc decrease from 29.8 to 22.5 emu/g and 696 to 328 Oe, respectively. The decrease of Ms results from the weakened Fe_A^{3+}-Fe_B^{3+} superexchange interactions and the increasing surface noncollinear layer. The change in coercivity can be explained by two factors. (1) The decreasing fraction of Co^{2+} at B site. Because Co^{2+} at the octahedral B site can raise the magnetocrystalline

anisotropy, which would increase the coercivity of spinel $CoFe_2O_4$ grains [17]. (2) The effect of grain sizes. Based on the XRD results, the decrease in grain sizes with the increase of Co^{2+} content results in the increase in the fraction of the small particles in which the superparamagnetic relaxation processes exists , which leads to the decreasing coercivity.

In summary, $Co_xFe_{3-x}O_4/SiO_2$ (x = 0.8, 0.9, 1.0 1.1) nanocomposites have been obtained by the sol-gel method. As the content of Co^{2+} increases from 0.8 to 1.1, the average particle size of $Co_xFe_{3-x}O_4$ in the sample decreases from 10.1 to 7.3 nm, while the lattice constant increases from 0.8361 to 0.8381 nm. TEM images of $Co_{0.8}Fe_{2.2}O_4$ sample show that spherical $Co_{0.8}Fe_{2.2}O_4$ nanocrystals with high crystallinity are surrounded by amorphous SiO_2 and have a size distribution. Mössbauer spectra results show that with increasing of Co^{2+} content, the hyperfine fields for both A and B-site decrease and the fraction of Co^{2+} occupying A-site increases. Moreover, the values of saturation magnetization and coercivity decrease with increasing Co^{2+} content. The weakened A-B interactions induced by the decrease in Fe^{3+} content will contribute to the decrease in the saturation magnetization, while the decreasing grain size and the variation of Co^{2+} at B-site result in the change in coercivity.

Acknowledgements This work was supported by the National Natural Science Foundation of China (Grant No. 21201078), Foundation of Science and Technology of Jilin, China (Grant No. 201205075), Foundation of Education Bureau of Jilin Province, China (Grant No. 2012182)

References

1. Mathieu, A., Lotfi Ben, T., Frédéric, H., Leila, S., Françoise, V., Nader, Y., Jean-Marc, G., Souad, A., Fernand, F.: Size-dependent magnetic properties of $CoFe_2O_4$ nanoparticles prepared in polyol. J. Phys., Condens. Mattter **23**, 506001 (2011)
2. Limaye, M.V., Singh, S.B., Date, S.K., Kothari, D., Reddy, V.R., Gupta, A., Sathe, V., Choudhary, R.J., Kulkarni, S.K.: High coercivity of oleic acid capped $CoFe_2O_4$ nanoparticles at room temperature. J. Phys. Chem. B **113**, 9070–9076 (2009)
3. Chinnasamy, C.N., Jeyadevan, B., Shinoda, K., Tohji, K., Djayaprawira, D.J., Takahashi, M., Joseyphus, R.J., Narayanasamy, A.: Unusually high coercivity and critical single-domain size of nearly monodispersed $CoFe_2O_4$ nanoparticles. Appl. Phys. Lett. **83**, 2862–2864 (2003)
4. Cannas, C., Musinu, A., Ardu, A., Orrù, F., Peddis, D., Casu, M., Sanna, R., Angius, F., Diaz, G., Piccaluga, G.: $CoFe_2O_4$ and $CoFe_2O_4/SiO_2$ core/shell nanoparticles: magnetic and spectroscopic study. Chem. Mater. **22**, 3353–3361 (2010)
5. Ayyappan, S., Mahadevan, S., Chandramohan, P., Srinivasan, M.P., Philip, J., Raj, B.: Influence of Co^{2+} ion concentration on the size, magnetic properties, and purity of $CoFe_2O_4$ spinel ferrite nanoparticles. J. Phys. Chem. C **114**, 6334–6341 (2010)
6. Shao, H., Huang, Y., Lee, H., Suh, Y.J., Kim, C.O.: Effect of PVP on the morphology of cobalt nanoparticles prepared by thermal decomposition of cobalt acetate. Curr. Appl. Phys. **6**(Supplement 1), e195–e197 (2006)
7. Pramanik, N.C., Fujii, T., Nakanishi, M., Takada, J.: Effect of Co^{2+} ion on the magnetic properties of sol-gel cobalt ferrite thin films. J. Mater. Chem. **14**, 3328–3332 (2004)
8. Cedeño-Mattei, Y., Perales-Pérez, O., Uwakweh, O.N.C.: Synthesis of high-coercivity non-stoichiometric cobalt ferrite nanocrystals: structural and magnetic characterization. Mater. Chem. Phys. **132**, 999–1006 (2012)
9. Zhang, S., Dong, D., Sui, Y., Liu, Z., Wang, H., Qian, Z., Su, W.: Preparation of core shell particles consisting of cobalt ferrite and silica by sol–gel process. J. Alloy. Compd. **415**, 257–260 (2006)
10. Praveena, K., Sadhana, K., Ramana Murthy, S.: Structural and magnetic properties of NiCuZn ferrite/SiO_2 nanocomposites. J. Magn. Magn. Mater. **323**, 2122–2128 (2011)

11. Woltersdorf, J., Nepijko, A.S., Pippel, E.: Dependence of lattice parameters of small particles on the size of the nuclei. Surf. Sci. **106**, 64–69 (1981)
12. Maaz, K., Mumtaz, A., Hasanain, S.K., Ceylan, A.: Synthesis and magnetic properties of cobalt ferrite ($CoFe_2O_4$) nanoparticles prepared by wet chemical route. J. Magn. Magn. Mater. **308**, 289–295 (2007)
13. Sreja, V., Vijayanand, S., Deka, S., Joy, P.A.: Magnetic and Mössbauer spectroscopic studies of NiZn ferrite nanoparticles synthesized by a combustion method. Hyperfine Interact. **183**, 99–107 (2008)
14. Sanchez, R.D., Rivas, J., Vaqueiro, P., Lopez-Quintela, M.A., Caeiro, D.: Particle size effects on magnetic properties of yttrium iron garnets prepared by a sol-gel method. J. Magn. Magn. Mater. **247**, 92–98 (2002)
15. Kumar, L., Kar, M.: Influence of Al^{3+} ion concentration on the crystal structure and magnetic anisotropy of nanocrystalline spinel cobalt ferrite. J. Magn. Magn. Mater. **323**, 2042–2048 (2011)
16. Lee, J.G., Park, J.Y., Kim, C.S.: Growth of ultra-fine cobalt ferrite particles by a sol–gel method and their magnetic properties. J. Magn. Magn. Mater. **33**, 3965–3968 (1998)
17. Bhide, V.G.: Mössbauer Effect and its Applications. Tata McGraw-Hill (1973)